JACS
JOURNAL OF THE AMERICAN CHEMICAL SOCIETY
Article
pubs.acs.org/JACS

UV-Induced Bursting of Cell-Sized Multicomponent Lipid Vesicles in a Photosensitive Surfactant Solution

Antoine Diguet,[†,‡,§] Miho Yanagisawa,[∥] Yan-Jun Liu,[†,‡,§] Elodie Brun,[†,‡,§] Sacha Abadie,[†,‡,§] Sergii Rudiuk,[†,‡,§] and Damien Baigl*[,†,‡,§]

[†]Department of Chemistry, Ecole Normale Supérieure, 24 rue Lhomond, 75005 Paris, France
[‡]Université Pierre et Marie Curie Paris 6, 4 place Jussieu, 75005 Paris, France
[§]UMR 8640, Centre National de la Recherche Scientifique, Paris, France
[∥]Department of Physics, Faculty of Sciences, Kyushu University, Fukuoka 812-8581, Japan

Supporting Information

ABSTRACT: We study the behavior of multicomponent giant unilamellar vesicles (GUVs) in the presence of AzoTAB, a photosensitive surfactant. GUVs are made of an equimolar ratio of dioleoylphosphatidylcholine (DOPC) and dipalmitoylphosphatidylcholine (DPPC) and various amounts of cholesterol (Chol), where the lipid membrane shows a phase separation into a DPPC-rich liquid-ordered (L_o) phase and a DOPC-rich liquid-disordered (L_d) phase. We find that UV illumination at 365 nm for 1 s induces the bursting of a significant fraction of the GUV population. The percentage of UV-induced disrupted vesicles, called bursting rate (Y_{burst}), increases with an increase in [AzoTAB] and depends on [Chol] in a non-monotonous manner. Y_{burst} decreases when [Chol] increases from 0 to 10 mol % and then increases with a further increase in [Chol], which can be correlated with the phase composition of the membrane. We show that Y_{burst} increases with the appearance of solid domains ([Chol] = 0) or with an increase in area fraction of L_o phase (with increasing [Chol] ≥ 10 mol %). Under our conditions (UV illumination at 365 nm for 1 s), maximal bursting efficiency (Y_{burst} = 53%) is obtained for [AzoTAB] = 1 mM and [Chol] = 40 mol %. Finally, by restricting the illumination area, we demonstrate the first selective UV-induced bursting of individual target GUVs. These results show a new method to probe biomembrane mechanical properties using light as well as pave the way for novel strategies of light-induced drug delivery.

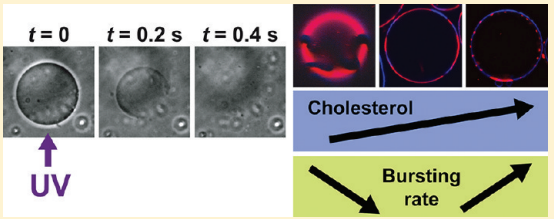

INTRODUCTION

Giant unilamellar vesicles (GUVs) are spherical entities with a diameter in the range 1−100 μm, which have attracted a growing interest for a large variety of biological and chemical applications.[1−3] GUVs made of lipids can be used as biomimetic cell-sized reactors[4−7] or model membrane systems.[8−12] In the latter case, multicomponent lipid membranes are particularly interesting for their similarity with biological membranes.[13−19] Since GUVs are large enough to allow direct microscopic observation of the membrane behavior, investigations have been carried out on morphological dynamics in response to various stimuli, such as temperature,[20] chemical reaction,[21] osmotic stress,[22−25] addition of detergent,[23,26] and magnetic field.[27] Light represents another particularly interesting stimulus as it offers high spatiotemporal resolution, excitation tunability, and contactless perturbation. The response of vesicles to light stimulation in the presence of various kinds of photosensitive molecules has been studied in the past few years, but it has been mainly limited to nonlipidic vesicles. For instance, in the case of catanionic small unilamellar vesicles (SUV), light has been used to trigger the disruption and the reformation of SUVs using a cationic[28−30] or an anionic[31] photosensitive surfactant. The light-induced disruption of GUVs containing a cationic photosensitive gemini surfactant[32,33] as well as of polymerosomes made of photosensitive diblock copolymers has also been reported.[34,35] In contrast, few studies have been devoted to the interaction between light and vesicles with a lipid membrane. In the case of SUVs, wavelength-dependent structures using photoisomerizable lipids[36−39] and light-induced permeation using photosentive surfactants[40,41] or a photoreticulable lipid[42] have been demonstrated. In the case of GUVs made of phospholipids, light-induced shape transitions in the presence of pyrene,[43] deformations,[44−46] and membrane phase separation[47] in vesicles containing a high concentration (≈40 mol %) of a photosensitive bolaphile in the membrane or permeability variations in the presence of a photosensitive amphiphilic polymer[48] have been reported. In this article, we report for the first time the effect of light applied on GUVs solely composed of natural lipids [dioleoylphosphatidylcholine (DOPC), dipalmitoylphosphatidylcholine (DPPC), cholesterol (Chol)] in the presence of a photosensitive azobenzene surfactant (AzoTAB) added to the outer medium of vesicles. We found that a short UV stimulation (365 nm for 1 s) induces immediate bursting of GUVs. We studied the effect of

Received: December 14, 2011
Published: February 8, 2012

   dx.doi.org/10.1021/ja211664f | J. Am. Chem. Soc. 2012, 134, 4898−4904

cholesterol content, wavelength of illumination, and AzoTAB concentration on the yield of bursting. We also applied local light stimulation for selective destruction of target individual GUVs among others.

RESULTS

Figure 1 shows our experimental system. We used an azobenzene trimethylammonium bromide surfactant (AzoTAB) as a photosensitive surfactant. Under dark conditions, AzoTAB is mainly in the trans configuration, which has a linear and apolar hydrophobic tail. Upon UV illumination (365 nm) *trans*-AzoTAB photoisomerizes into cis configuration, which has a bent and more polar tail. *cis*-AzoTAB is stable and can be kept under dark conditions for several hours.[49] The system is reversible, and *cis*-AzoTAB isomerizes back to trans configuration upon blue light (475 nm) illumination (Figure 1A). AzoTAB has been mainly used for the photocontrol of surface tension,[50,51] DNA conformation,[49,52,53] and gene expression systems.[54−56] Here, we investigated how light affected the behavior of lipid GUVs in the presence of AzoTAB. For all experiments the GUV membrane was composed of an equimolar mixture of DOPC and DPPC and different fractions of Chol, which is a standard composition for a multicomponent model membrane system.[16] At room temperature, in the absence of cholesterol, DPPC is in the gel phase and forms solid domains, as shown in Figure 1B (left), where rhodamine-DPPE (red) and perylene (blue) are both excluded from the noncircular, solid domains. In the presence of cholesterol ([Chol] ≥ 10 mol %), the membrane separates into two phases: a DPPC- and Chol-rich liquid-ordered (L_o) phase and a DOPC-rich liquid-disordered (L_d) phase, as shown in Figure 1B (right), where rhodamine-DPPE (red) and perylene (blue) are localized in L_d and L_o phases, respectively.[15] GUVs were prepared by electroformation in a 0.1 M sucrose solution. After electroformation, GUVs were mixed with an AzoTAB solution in glucose having the same osmolarity as that of the sucrose solution. After 2 h of sedimentation due to weight density difference between sucrose and glucose, most of vesicles were collected at the bottom of a chamber and observed by phase contrast microscopy, before and after illumination by UV (365 nm) or blue (475 nm) light for 1 s (Figure 1C).

We first observed that the application of UV on GUVs in the presence of AzoTAB resulted in the bursting of a significant fraction of GUVs (Figure 2A and movie S1, Supporting Information). Time lapse observations of individual bursting events showed that bursting typically occurs within a few hundreds of milliseconds (Figure 2B). To our knowledge, this

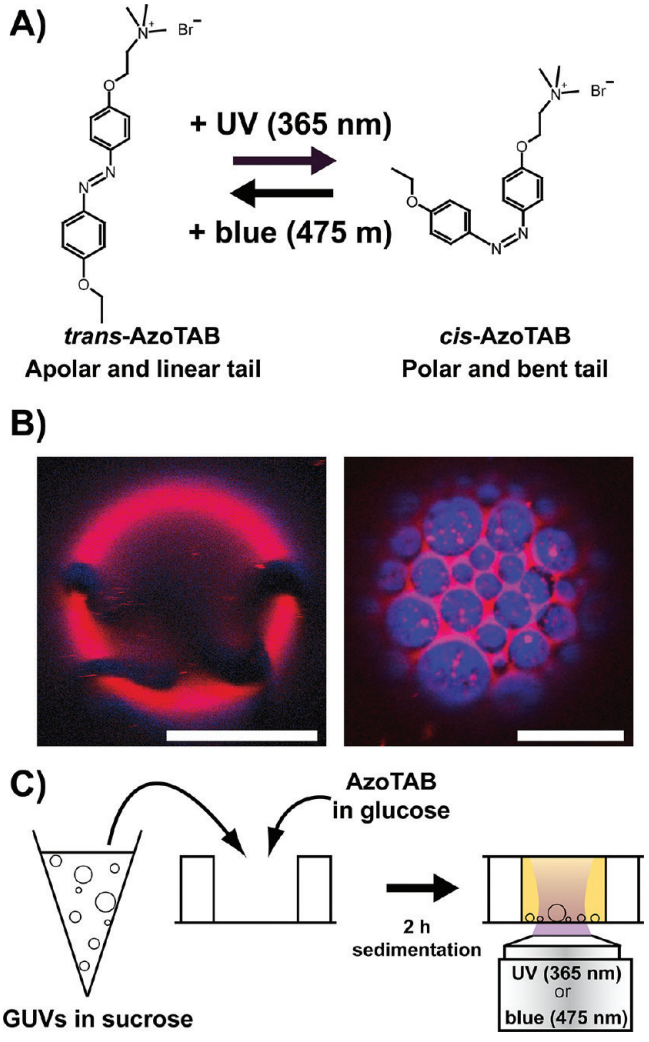

Figure 1. Light stimulation of multicomponent giant unilamellar vesicles (GUVs) in the presence of AzoTAB photosensitive surfactant. (A) Molecular structure and photoisomerization of AzoTAB. Upon UV illumination at λ = 365 nm, AzoTAB isomerizes to cis configuration, resulting in a more polar and bent tail. The process is reversible upon visible light illumination at λ = 475 nm, resulting in the isomerization into trans configuration. (B) Confocal microscopy images of GUVs made of 1:1 DOPC/DPPC with [Chol] = 0 and 10 mol % (left and right, respectively). Domains in liquid-disordered (L_d) and liquid-ordered (L_o) phase are labeled in red using rhodamine-DPPE (2 mol %) and blue using perylene (0.5 mol %), respectively. Dark regions in the left picture indicate a solid phase where both dyes are fully excluded. Scale bars are 10 μm. (C) A suspension of GUVs in sucrose is mixed with an AzoTAB solution in glucose having the same osmolarity. After 2 h of sedimentation, GUVs are observed and illuminated by UV (365 nm) or blue (475 nm) light for 1 s using an inverted microscope.

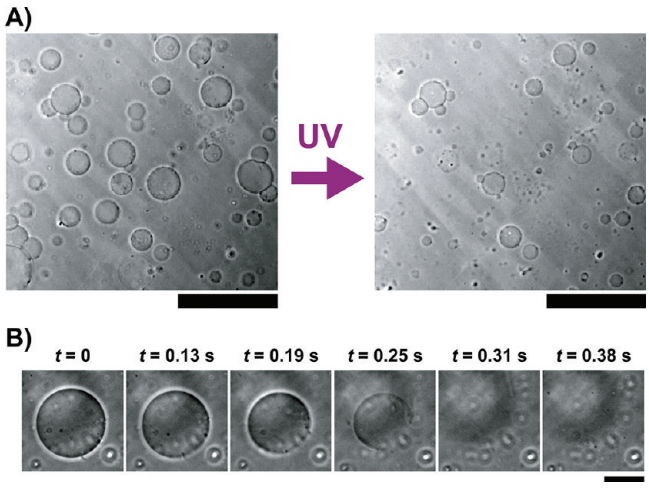

Figure 2. UV-induced bursting of GUVs. (A) Phase contrast microscopy images of GUVs made of 1:1 DOPC/DPPC and cholesterol (40 mol %) in the presence of AzoTAB (1 mM), before (left) and after (right) application of UV (365 nm for 1 s). Scale bar is 200 μm. (B) Timelapse observation by phase contrast microscopy of an individual GUV under an UV illumination (365 nm) started at t = 0. Scale bar is 30 μm.

dx.doi.org/10.1021/ja211664f | J. Am. Chem. Soc. 2012, 134, 4898−4904

is the first time that UV-induced bursting of GUVs solely composed of lipids is reported.

We then systematically measured the bursting rate, Y_{burst}, defined as the percentage of GUVs that were destroyed by UV illumination (365 nm for 1 s). Figure 3 shows Y_{burst} as function

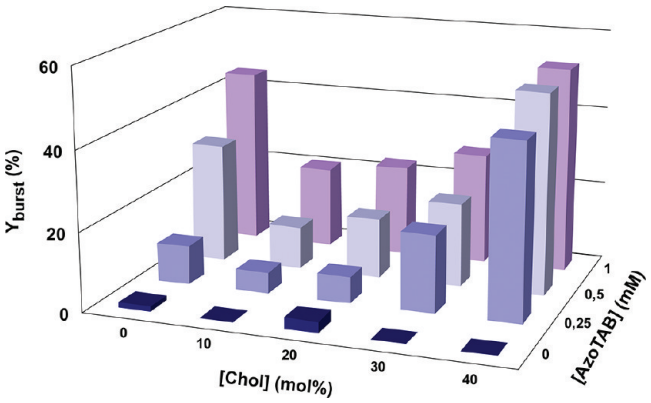

Figure 3. Effect of AzoTAB and cholesterol on UV-induced bursting rate. Percentage of GUVs disrupted after UV illumination (365 nm for 1 s), called bursting rate (Y_{burst}), as a function of AzoTAB concentration and cholesterol (Chol) composition of the membrane.

of cholesterol fraction in the membrane ([Chol]) and AzoTAB concentration in the outer medium of vesicles ([AzoTAB]). Figure 3 shows that regardless of cholesterol content, AzoTAB has a strong influence on the yield of bursting. Without AzoTAB, most of vesicles remain intact after UV illumination ($Y_{burst} \leq 3\%$). In contrast, in the presence of AzoTAB, a significant fraction of vesicles burst upon UV illumination, and Y_{burst} increases with an increase in [AzoTAB]. This shows that under our experimental conditions, AzoTAB is needed for UV-induced bursting. Notably, Figure 3 shows also a non-monotonous behavior as a function of cholesterol content. Regardless of [AzoTAB] $\geq$ 0.25 mM, Y_{burst} shows a marked drop when [Chol] increases from 0 to 10 mol % and then increases when [Chol] increases from 10 to 40 mol %. All these results show that the presence of both AzoTAB and membrane composition have a role in the extent of bursting upon UV illumination. The maximum bursting rate is 53%, which is obtained for [AzoTAB] = 1 mM and [Chol] = 40 mol %.

DISCUSSION

We showed that AzoTAB had a critical role in both occurrence and extent of UV-induced bursting. To correlate this effect with the isomerization properties of AzoTAB, we studied the effect of AzoTAB configuration (cis or trans) and isomerization (cis−trans or trans−cis) on illumination-induced bursting under conditions where maximal bursting rate was observed ([AzoTAB] 1 mM, [Chol] = 40 mol %). First, AzoTAB solution was exposed to UV to get *cis*-AzoTAB in solution prior to addition to GUVs in the dark. When UV (365 nm for 1 s) was applied, AzoTAB remained in the cis configuration, and no bursting was observed (Figure 4A, left and middle). This shows that UV illumination by itself does not induce GUV bursting. When blue light (475 nm for 1 s) was applied on the same sample, *cis*-AzoTAB isomerized to trans configuration, and no bursting was observed (Figure 4A, middle and right). This shows that cis−trans isomerization is not responsible of bursting. We then added *trans*-AzoTAB solution to a new GUV solution. When blue light was applied, AzoTAB remained

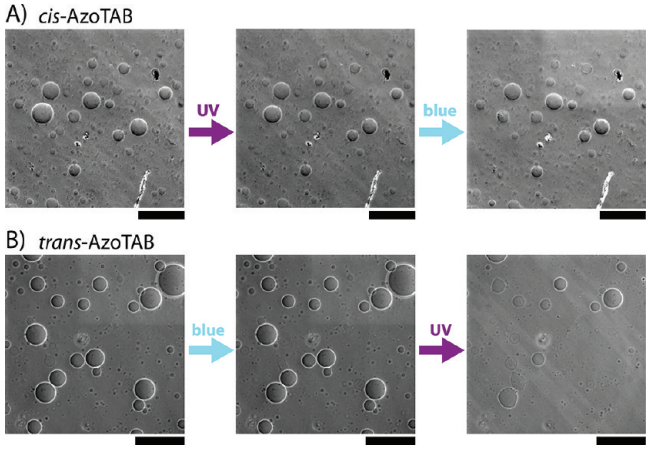

Figure 4. Effect of UV and blue light illumination in the presence of *cis*- or *trans*-AzoTAB. Phase contrast microscopy images of GUVs before and after UV (365 nm for 1 s) or blue (475 nm for 1 s) illumination initially in the presence of (A) *cis*-AzoTAB or (B) *trans*-AzoTAB. GUVs are made of 1:1 DOPC/DPPC and 40 mol % cholesterol, with [AzoTAB] = 1 mM. Scale bars are 200 μm.

in trans configuration, and no bursting was observed (Figure 4B, left and middle). This shows that illumination-induced bursting in the presence of AzoTAB is dependent on wavelength illumination and is not due to a thermal effect. When UV was applied on this sample, *trans*-AzoTAB isomerized to cis configuration, and the usual UV-induced bursting was observed (Figure 4B, middle and right). All these results show that both the presence of *trans*-AzoTAB in the initial solution and UV-induced trans−cis isomerization are necessary to observe UV-induced bursting.

The role of the configuration of AzoTAB (trans or cis) might be attributed to different affinities for the GUV membrane between trans and cis isomers. To assess the insertion of AzoTAB in GUV membrane and compare the affinities between trans and cis isomers, we performed UV−vis spectroscopy measurements on GUVs prepared under the conditions of maximal bursting ([AzoTAB] = 1 mM and [Chol] = 40 mol %). GUVs were first incubated with AzoTAB (1 mM), then concentrated by centrifugation, washed with glucose to remove most of AzoTAB from the bulk solution, and concentrated again by centrifugation (Figure 5A). Figure 5B,C shows the UV−vis spectra for *trans*- and *cis*-AzoTAB, respectively. Both isomers have spectra similar to those measured in pure water[53] with a characteristic maximum at 354 nm for trans and 319 and 430 nm for cis. The absorbance values for the lower phase in the absence of GUVs and for the upper phase are very similar and approximately correspond to the remaining amount of AzoTAB in the outer medium of GUVs after washing. Interestingly, in the case of *trans*-AzoTAB (Figure 5B), the lower phase in the presence of GUVs shows a significantly higher absorption, which shows that GUV membranes have accumulated *trans*-AzoTAB during incubation. Moreover, UV application on this sample induces the isomerization from trans to cis isomer (Figure S1, Supporting Information), which shows that, under our experimental conditions, UV-induced isomerization occurs in the membrane. A very different situation is observed with *cis*-AzoTAB (Figure 5C), where the absorption of the lower phase in the presence of GUVs is very similar to the control experiments (lower phase in the absence of GUV and upper phase with GUVs). This shows

dx.doi.org/10.1021/ja211664f | J. Am. Chem. Soc. 2012, 134, 4898−4904

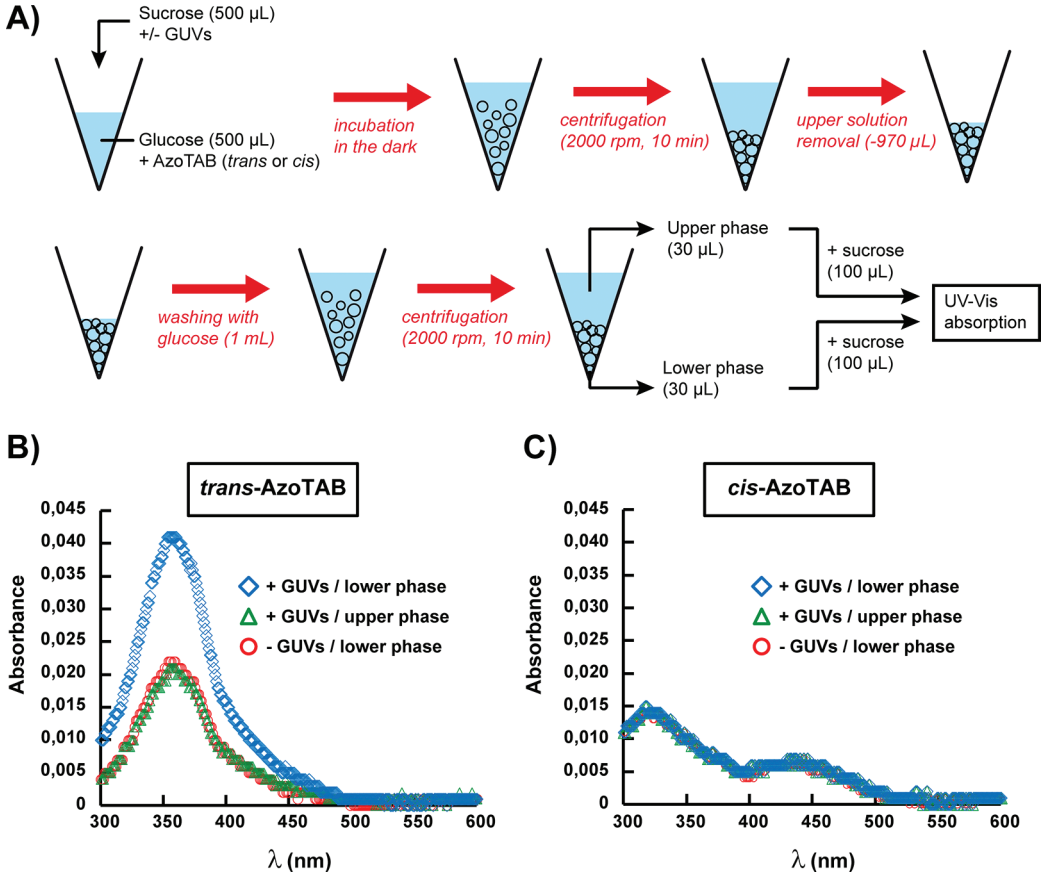

Figure 5. Characterization of AzoTAB insertion in GUV membrane by UV−vis spectroscopy. (A) 500 μL of a sucrose solution (0.1 M) with or without GUVs is mixed with 500 μL of glucose (0.1 M) containing AzoTAB (2 mM), incubated for 30 min in the dark, and centrifuged at 2000 rpm for 10 min prior to removal of the upper phase solution. The lower phase is then washed with 1 mL of glucose (0.1 M) and centrifuged at 2000 rpm for 10 min. To establish the UV−vis absorption spectra, 30 μL of the lower or upper phase is mixed with 100 μL of sucrose (0.1 M). Sucrose/glucose with or without AzoTAB are adjusted to have the same osmolarity. (B−C) UV−vis absorption spectra of the lower and upper phases, in the presence or absence of GUVs for (B) *trans*-AzoTAB and (C) *cis*-AzoTAB, respectively.

that we could not detect any significant accumulation of *cis*-AzoTAB in GUV membranes. The different affinities for membranes between *trans*- and *cis*-AzoTAB can be explained as follows. The tail of *trans*-AzoTAB is apolar and more hydrophobic than that of *cis*-AzoTAB (Figure 1A), which is confirmed by critical micellar concentrations (CMC) measurements (CMC = 12.6 and 14.6 mM for trans and cis isomers, respectively).[53] Moreover, *trans*-AzoTAB has a linear tail, while *cis*-AzoTAB has a bent configuration. As a result, *trans*-AzoTAB is more prone to insert in the hydrophobic bilayered membrane of GUVs. If *cis*-AzoTAB has no or few interaction with the GUV membrane, UV or visible light illumination has almost no effect on GUVs initially in the presence of *cis*-AzoTAB (Figure 4A). In contrast, *trans*-AzoTAB is hydrophobic enough to insert in GUV membrane without disrupting it. Consequently, blue light has no effect (no isomerization), but UV induces a trans to cis isomerization of all AzoTAB molecules, including those inserted in the membrane (Figure S1, Supporting Information). The isomerization of AzoTAB inside GUV membrane may disturb the organization of phospholipid to an extent that is sufficient to induce membrane rupture and vesicle bursting (Figures 2,3,4B).

Since the perturbation of the phospholipid organization seems to be responsible for the GUV bursting, it is interesting to see how this effect is affected by the membrane composition. In our experiments, we kept an equimolar ratio of DOPC/DPPC and varied the fraction of cholesterol from 0 to 40 mol %. Figure 3 shows that cholesterol fraction has a dramatic effect on the bursting rate. In the absence of cholesterol, DPPC is in the gel phase and forms solid domains (Figure 1B, left). In contrast, in the presence of a small fraction of cholesterol ([Chol] = 10 mol %), there is no solid domain anymore, and the GUV membrane shows two coexisting liquid phases: a DPPC- and Chol-rich L_o phase that is shown in blue, and a DOPC-rich L_d phase that is shown in red (Figure 1B, right), which is in agreement with previous reports on DOPC/DPPC/Chol systems.[14,16,57] Interestingly, this transition in DPPC-rich phase from gel phase to L_o phase is accompanied by a sharp drop in bursting rate (Figure 3). For instance, when [Chol] increases from 0 to 10 mol %, Y_{burst} drops from 30% and 45% to 11% and 21% for [AzoTAB] = 0.5 mM and 1 mM, respectively. Saturated lipids, such as DPPC, in gel phase are known to have a high area compressibility modulus ($K_A \approx 800$ mN·m^{-1}),[58] while for DOPC in a liquid phase $K_A \approx 250$ mN·m^{-1}.[59] The presence of a small amount of cholesterol disrupts the long-range lateral order of DPPC lipids in solid domains, which fluidizes the membrane and induces a decrease in K_A ($K_A \approx 400$ mN·m^{-1} for DPPC vesicles with [Chol] $\leq$ 15 mol %).[60] We can thus suggest that, in response to AzoTAB isomerization, phospholipids present in a liquid-state membrane, that is, in the presence of a small amount of cholesterol, reorganize more easily than when solid domains exist. As a result, GUVs are

dx.doi.org/10.1021/ja211664f | J. Am. Chem. Soc. 2012, 134, 4898−4904

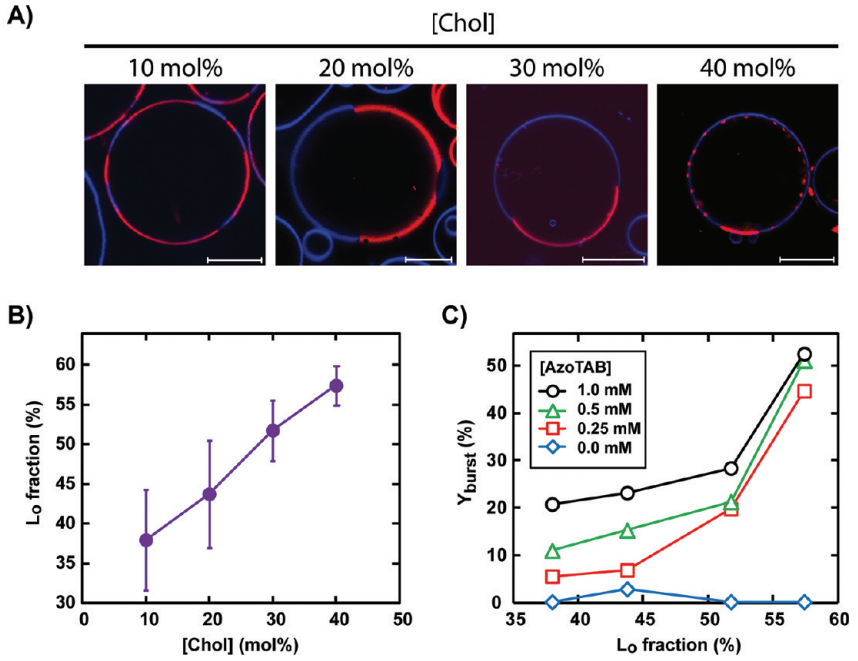

Figure 6. Effect of membrane phase composition. (A) Confocal microscopy images of GUVs composed of 1:1 DOPC/DPPC and various fractions of cholesterol (Chol). Domains in L_d and L_o phases are labeled in red using rhodamine-DPPE (2 mol %) and blue using perylene (0.5 mol %), respectively. Scale bars are 10 μm. (B) Area fraction of L_o phase in GUVs composed of 1:1 DOPC/DPPC and cholesterol, as a function of cholesterol fraction. (C) Bursting rate (Y_{burst}) as a function of the fraction of L_o phase in GUVs for various AzoTAB concentrations.

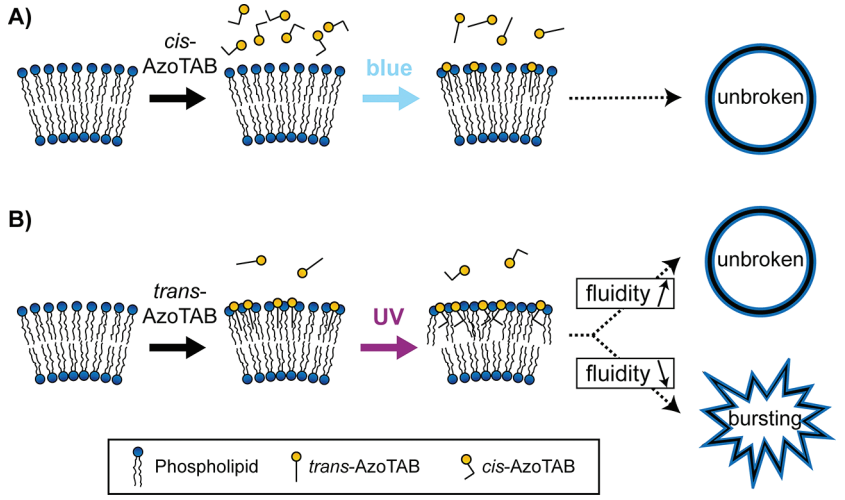

Figure 7. Suggested mechanism. (A) *cis*-AzoTAB does not insert in the membrane, and blue light-induced cis−trans isomerization does not affect membrane stability. (B) *trans*-AzoTAB is hydrophobic enough to insert in the membrane. UV-induced trans−cis isomerization disturbs phospholipid organization and leads to GUV bursting when the membrane is not fluid enough (presence of solid domains in the absence of cholesterol or high fraction of L_o phase at high cholesterol concentration).

more prone to UV-induced bursting when the membrane does not contain cholesterol, that is, when solid domains exist. In the presence of cholesterol, the opposite trend is observed. The bursting rate increases with an increase in cholesterol content (Figure 3). To better understand this effect, we observed a large number of GUVs by confocal microscopy (Figure 6A) and estimated the area fraction of L_o phase (Figure 6B) as a function of [Chol]. Figure 6A,B shows that the area fraction of L_o phase increases from 38 ± 6% to 57 ± 2% when [Chol] increases from 10 to 40 mol %, which is in agreement with former reports.[14,16,57] It is thus interesting to correlate the bursting yield with the fraction of L_o phase. Figure 6C shows that almost no bursting occurs in the absence of AzoTAB, which confirms that AzoTAB is needed for bursting to occur. For a given fraction in L_o phase, Y_{burst} increases with an increase in AzoTAB concentration. Phospholipids have to reorganize in response to the UV-induced isomerization of AzoTAB, and the increase in Y_{burst} with [AzoTAB] can be attributed to a higher perturbation when AzoTAB concentration increases. Interestingly, Figure 6C also shows that in the presence of AzoTAB, the bursting yield increases with an increase in fraction of L_o phase, regardless of AzoTAB concentration. This effect can be attributed to the lower fluidity of the L_o phase ($K_A \approx 1100-1300$ mN·m^{-1} for DPPC vesicles with [Chol] = 20−40 mol %)[60] compared to the L_d phase ($K_A \approx 250$ mN·m^{-1} for pure DOPC).[59] Phospholipids reorganization in response to the UV-

dx.doi.org/10.1021/ja211664f | J. Am. Chem. Soc. 2012, 134, 4898−4904

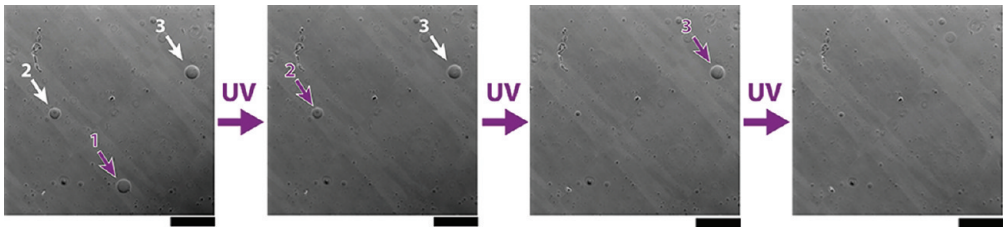

Figure 8. Selective UV-induced bursting of individual target GUVs. Phase contrast microscopy images of GUVs made of 1:1 DOPC/DPPC containing 40 mol % cholesterol in the presence of AzoTAB (1 mM). GUVs pointed by arrows were successively illuminated by a single UV illumination pulse (365 nm for 1 s) having a diameter of about 300 μm centered on the target GUV. Scale bars are 200 μm.

induced isomerization of AzoTAB is probably facilitated when the membrane is more fluid, that is, in the presence of a low fraction of L_o phase. This could explain the increase in Y_{burst} with an increase in area fraction of L_o phase.

Figure 7 summarizes the possible mechanism explaining UV-induced bursting in the presence of *trans*-AzoTAB and its dependence on cholesterol fraction; *cis*-AzoTAB, which is less hydrophobic than *trans*-AzoTAB, does not insert in the GUV membrane, and blue light illumination does not induce any bursting (Figure 7A). In contrast, *trans*-AzoTAB is hydrophobic enough to insert in the membrane. When UV light is applied, trans−cis isomerization disturbs the lipid organization, which results in GUV bursting when the membrane is not fluid enough to reorganize, that is, in the presence of solid domains ([Chol] = 0) or when a high fraction of L_o phase is present in the membrane (high cholesterol concentration) (Figure 7B).

Since UV-induced bursting is related to the local isomerization of AzoTAB in the GUV membrane, we studied the response to the selective illumination of individual target GUVs among others. To this end, UV illumination was performed through a high-magnification objective lens (100×) to get an illumination area of about 300 μm in diameter. The illumination was applied on a highly diluted suspension of GUVs (10× more diluted than in former experiments) so that the illumination area affects no more than one target GUV. Figure 8 shows typical observations for GUVs composed of 40 mol % of cholesterol, which are the most sensitive to UV illumination, according to Figure 3, exposed one by one to a single UV illumination pulse (365 nm for 1 s). The first UV pulse was applied to GUV "number 1", which resulted in the specific bursting of the target GUV while other GUVs in the observation field remained intact. The same operation was repeated successively to GUV "numbers 2 and 3" and resulted each time in the selective bursting of the target vesicle. To our knowledge, this is the first time that controlled bursting of target individual GUVs among others is reported. Our light stimulation thus enables both a fast response and a good spatial resolution.

■ CONCLUSION

We have reported for the first time the use of UV light to induce the bursting of multicomponent GUVs. This was achieved with GUVs composed of 1:1 DOPC/DPPC and various fractions of cholesterol in the presence of AzoTAB photosensitive surfactant. We found that bursting was particularly efficient in the absence of cholesterol or with high cholesterol concentration. This non-monotonous cholesterol effect was attributed to the role of membrane fluidity, which modulates the ability of phospholipids to reorganize in response to AzoTAB isomerization after the UV light stimulus. The UV-induced response was demonstrated to be fast (less than 1 s) and spatially resolved, which allowed us to control for the first time the bursting of individual target GUVs among others. In the future, these results could be applied to locally probe biomembrane fluidity using light. It can also be useful for the light-triggered release of solutes from artificial cell systems.

■ ASSOCIATED CONTENT

Supporting Information

Materials and methods, Figure S1, movie S1, and movie legend. This material is available free of charge via the Internet at http://pubs.acs.org.

■ AUTHOR INFORMATION

Corresponding Author

damien.baigl@ens.fr

Notes

The authors declare no competing financial interest.

■ ACKNOWLEDGMENTS

The research leading to these results has received funding from the European Research Council under the European Community's Seventh Framework Programme (FP7/2007 2013)/ERC grant agreement no. 258782 and from Institut Universitaire de France.

■ REFERENCES

(1) Lasic, D. D. *Liposomes in Gene Delivery*; CRC Press: Boca Raton, FL, 1987.
(2) Luisi, P. L.; Walde, P. *Giant Liposomes, Perspectives in Supramolecular Chemistry*; John Wiley and Sons Ltd.: New York, 2000.
(3) Walde, P.; Cosentino, K.; Engel, H.; Stano, P. *ChemBioChem* **2010**, *11*, 848−865.
(4) Karlsson, A.; Karlsson, R.; Karlsson, M.; Cans, A. S.; Stromberg, A.; Ryttsen, F.; Orwar, O. *Nature* **2001**, *409*, 150−152.
(5) Noireaux, V.; Libchaber, A. *Proc. Natl. Acad. Sci. U.S.A.* **2004**, *101*, 17669−17694.
(6) Chen, I. A.; Salehi-Ashtiani, K.; Szostak, J. W. *J. Am. Chem. Soc.* **2005**, *127*, 13213−13219.
(7) Saito, H.; Kato, Y.; Le Berre, M.; Yamada, A.; Inoue, T.; Yoshikawa, K.; Baigl, D. *ChemBioChem* **2009**, *10*, 1640−1643.
(8) Limozin, L.; Roth, A.; Sackmann, E. *Phys. Rev. Lett.* **2005**, *95*, 178101.
(9) Römer, W.; Berland, L.; Chambon, V.; Gaus, K.; Windschiegl, B.; Tenza, D.; Aly, M. R. E.; Fraisier, V.; Florent, J.-C.; Perrais, D.; Lamaze, C.; Raposo, G.; Steinem, C.; Sens, P.; Bassereau, P.; Johannes, L. *Nature* **2007**, *450*, 670.
(10) Osawa, M.; Anderson, D. E.; Erickson, H. P. *Science* **2008**, *320*, 792−294.
(11) Merkle, D.; Kahya, N.; Schwille, P. *ChemBioChem* **2008**, *9*, 2673−2681.

(12) Pontani, L.-L.; Van der Gucht, J.; Salbreux, G.; Heuvingh, J.; Joanny, J.-F.; Sykes, C. *Biophys. J.* **2009**, *96*, 192−198.
(13) Dietrich, C.; Bagatolli, L. A.; Volovyk, Z. N.; Thompson, N. L.; Levi, M.; Jacobson, K.; Gratton, E. *Biophys. J.* **2001**, *80*, 1417−1428.
(14) Veatch, S. L.; Keller, S. L. *Phys. Rev. Lett.* **2002**, *89*, 268101.
(15) Baumgart, T.; Hess, S. T.; Webb, W. W. *Nature* **2003**, *425*, 821−824.
(16) Veatch, S. L.; Keller, S. L. *Biophys. J.* **2003**, *85*, 3074−3083.
(17) Collins, M. D.; Keller, S. L. *Proc. Natl. Acad. Sci. U.S.A.* **2008**, *105*, 124−128.
(18) Yu, Y.; Vroman, J. A.; Bae, S. C.; Granick, S. *J. Am. Chem. Soc.* **2010**, *132*, 195−201.
(19) Van den Bogaart, G.; Meyenberg, K.; Risselada, H. J.; Amin, H.; Willig, K. I.; Hubrich, B. E.; Dier, M.; Hell, S. W.; Grubmüller, H.; Diederichsen, U.; Jahn, R. *Nature* **2011**, *479*, 552−555.
(20) Käs, J.; Sackmann, E. *Biophys. J.* **1991**, *60*, 825−844.
(21) Petrov, P. G.; Lee, J. B.; Döbereiner, H.-G. *Europhys. Lett.* **1999**, *48*, 435−441.
(22) Bernard, A. L.; Guedeau-Boudeville, M. A.; Jullien, L.; Di Meglio, J. M. *Biochim. Biophys. Acta, Biomembr.* **2002**, *1567*, 1−5.
(23) Hamada, T.; Miura, Y.; Ishii, K.; Araki, S.; Yoshikawa, K.; Vestergaard, M.; Takagi, M. *J. Phys. Chem. B* **2007**, *111*, 10853−10857.
(24) Long, M. S.; Cans, A. S.; Keating, C. D. *J. Am. Chem. Soc.* **2008**, *130*, 756−762.
(25) Yanagisawa, M.; Imai, M.; Taniguchi, T. *Phys. Rev. Lett.* **2008**, *100*, 148102.
(26) Staneva, G.; Seigneuret, M.; Koumanov, K.; Trugnan, G.; Angelova, M. I. *Chem. Phys. Lipids* **2005**, *136*, 55−66.
(27) Ménager, C.; Guemghar, D.; Perzynski, R.; Lesieur, S.; Cabuil, V. *Langmuir* **2008**, *24*, 4968−4974.
(28) Sakai, H.; Matsumura, A.; Yokoyama, S.; Saji, T.; Abe, M. *J. Phys. Chem. B* **1999**, *103*, 10737−10740.
(29) Hubbard, F. P. Jr.; Santonicola, G.; Kaler, E. W.; Abbott, N. L. *Langmuir* **2005**, *21*, 6131−6136.
(30) Hubbart, F. P. Jr.; Abbott, N. L. *Langmuir* **2007**, *23*, 4819−4829.
(31) Eastoe, J.; Vesperinas, A.; Donnewirth, A.-C.; Wyatt, P.; Grillo, I.; Heenan, R. K.; Davis, S. *Langmuir* **2006**, *22*, 851−853.
(32) Faure, D.; Gravier, J.; Labrot, T.; Desbat, B.; Oda, R.; Bassani, D. M. *Chem. Commun.* **2005**, 1167−1169.
(33) Ahmad, R. K.; Faure, D.; Goddard, P.; Oda, R.; Bassani, D. M. *Org. Biomol. Chem.* **2009**, *7*, 3173−3178.
(34) Su, W.; Han, K.; Luo, Y.; Wang, Z.; Li, Y.; Zhang, Q. *Macromol. Chem. Phys.* **2007**, *208*, 955−963.
(35) Mabrouk, E.; Cuvelier, D.; Brochard-Wyart, F.; Nassoy, P.; Li, M.-H. *Proc. Natl. Acad. Sci. U.S.A.* **2009**, *106*, 7294−7298.
(36) Song, X.; Geiger, C.; Vaday, S.; Perlstein, J.; Whitten, D. G. J. *Photochem. Photobiol. A* **1996**, *102*, 39−45.
(37) Song, X.; Perlstein, J.; Whitten, D. G. *J. Am. Chem. Soc.* **1997**, *119*, 9144−9159.
(38) Whitten, D. G.; Chen, L.; Geiger, H. C.; Perlstein, J.; Song, X. *J. Phys. Chem. B* **1998**, *102*, 10098−10111.
(39) Uda, R. M.; Hiraishi, E.; Ohnishi, R.; Nakahara, Y.; Kimura, K. *Langmuir* **2010**, *26*, 5444−5450.
(40) Lei, Y.; Hurst, J. K. *Langmuir* **1999**, *15*, 3424−3429.
(41) Kuiper, J. M.; Engberts, J. B. F. N. *Langmuir* **2004**, *20*, 1152−1160.
(42) Shum, P.; Kim, J.-M.; Thompson, D. H. *Adv. Drug Delivery Rev.* **2001**, *53*, 273−284.
(43) Brückner, E.; Sonntag, P.; Rehage, H. *Langmuir* **2001**, *17*, 2308−2311.
(44) Hamada, T.; Sato, Y. T.; Yoshikawa, K.; Nagasaki, T. *Langmuir* **2005**, *21*, 7626−7628.
(45) Ishii, K.; Hamada, T.; Hatakeyama, M.; Sugimoto, R.; Nagasaki, T.; Takagi, M. *ChemBioChem* **2009**, *10*, 251−256.
(46) Hamada, T.; Sugimoto, R.; Vestergaard, M. C.; Nagasaki, T.; Takagi, M. *J. Am. Chem. Soc.* **2010**, *132*, 10528−10632.
(47) Hamada, T.; Sugimoto, R.; Nagasaki, T.; Takagi, M. *Soft Matter* **2011**, *7*, 220−224.
(48) Sebai, S. C.; Cribier, S.; Karimi, A.; Massotte, D.; Tribet, C. *Langmuir* **2010**, *26*, 14135−14141.
(49) Le Ny, A.-L. M.; Lee, C. T. Jr. *J. Am. Chem. Soc.* **2006**, *128*, 6400−6408.
(50) Diguet, A.; Guillermic, R.-M.; Magome, N.; Saint-Jalmes, A.; Chen, Y.; Yoshikawa, K.; Baigl, D. *Angew. Chem., Int. Ed.* **2009**, *48*, 9281−9284.
(51) Diguet, A.; Hao, L.; Queyriaux, N.; Chen, Y.; Baigl, D. *Lab Chip* **2011**, *11*, 2666−2669.
(52) Sollogoub, M.; Guieu, S.; Geoffroy, M.; Yamada, A.; Estévez-Torres, A.; Yoshikawa, K.; Baigl, D. *ChemBioChem* **2008**, *9*, 1201−1206.
(53) Diguet, A.; Mani, N. K.; Geoffroy, M.; Sollogoub, M.; Baigl, D. *Chem.—Eur. J.* **2010**, *16*, 11890−11896.
(54) Estévez-Torres, A.; Crozatier, C.; Diguet, A.; Hara, T.; Saito, H.; Yoshikawa, K.; Baigl, D. *Proc. Natl. Acad. Sci. U.S.A.* **2009**, *106*, 12219−12223.
(55) Estévez-Torres, A.; Baigl, D. *Soft Matter* **2011**, *7*, 6746−6756.
(56) Rudiuk, S.; Saito, H.; Hara, T.; Inoue, T.; Yoshikawa, K.; Baigl, D. *Biomacromolecules* **2011**, *12*, 3945−3951.
(57) Yanagisawa, M.; Shimokawa, N.; Ichikawa, M.; Yoshikawa, K. *Soft Matter* **2012**, *8*, 488−495.
(58) Needham, D.; Evans, E. *Biochemistry* **1988**, *27*, 8261−8269.
(59) Rawicz, W.; Olbrich, K. C.; McIntosh, T.; Needham, D.; Evans, E. *Biophys. J.* **2000**, *79*, 328−339.
(60) Tierney, K. J.; Block, D. E.; Longo, M. L. *Biophys. J.* **2005**, *89*, 2481−2493.